

Computer-Controlled 3D Surface Weaving

Xiangjia Chen^{1,2}, Lip M. Lai², Zishun Liu², Isaac C.W. Leung², Charlie C.L. Wang^{3*} and Yeung Yam^{1,2*}

Abstract—In this paper, we present a new computer-controlled weaving system that enables the fabrication of woven fabrics in 3D freeform surfaces by using threads in non-traditional materials with high bending-stiffness. Conventional flat weaving technique is extended by the principle of short-row shaping to form 3D woven structures in freeform surfaces. A new weaving mechanism and its numerical control system are investigated to realize the function of 3D surface weaving. To guide the operation of this system, a software solution is developed to convert a given 3D freeform surface into the corresponding weaving operations (indicated as W-code) with the help of the short-row knitting map generation method. A variety of examples have been fabricated by our prototype system to demonstrate their functionality in different applications.

Index Terms—3D surface weaving, non-traditional material, high bending-stiffness, weaving machine

I. INTRODUCTION

The history of textile fabrication is probably as old as human history [1]. With the development of civilization, the function of textile products has been extended from keeping warmth to smart wearable devices in applications such as aerospace engineering [2] and biomedical engineering [3]. There are growing demands for the 3D shape control of new composite materials [4] and e-textile [5], [6], where the geometry of fabrics can possibly be formed by three different forming methods including knitting [7]–[10], weaving [11]–[13], felting [14] and robotic deposition / winding [15]–[17].

Among these techniques, threads / fibres are randomly distributed in the resultant fabrics of felting (see the lower right of Fig.1). The approaches of robotic direct deposition have low efficiency – i.e., the threads are deposited one by one in a manner similar to filament based 3D printing [15], [16], and the winding technique is mainly limited to the surfaces obtained by revolution [17], [18]. Given stitches as the basic building blocks of textile, it is expected to control the location of threads by designing the distribution of stitches. Note that, for the sake of explanation, we simply call each unit structure of woven fabrics as a *stitch* in the rest of this paper. The bottom row of Fig.1 shows the stitch structures in weaving (left), in knitting (middle), and the unstructured threads in felting (right). Generally, all structured stitches need to be mapped into the elements of a two-dimensional grid layout to enable the manufacturing process. Specifically, the map for a planar 2D

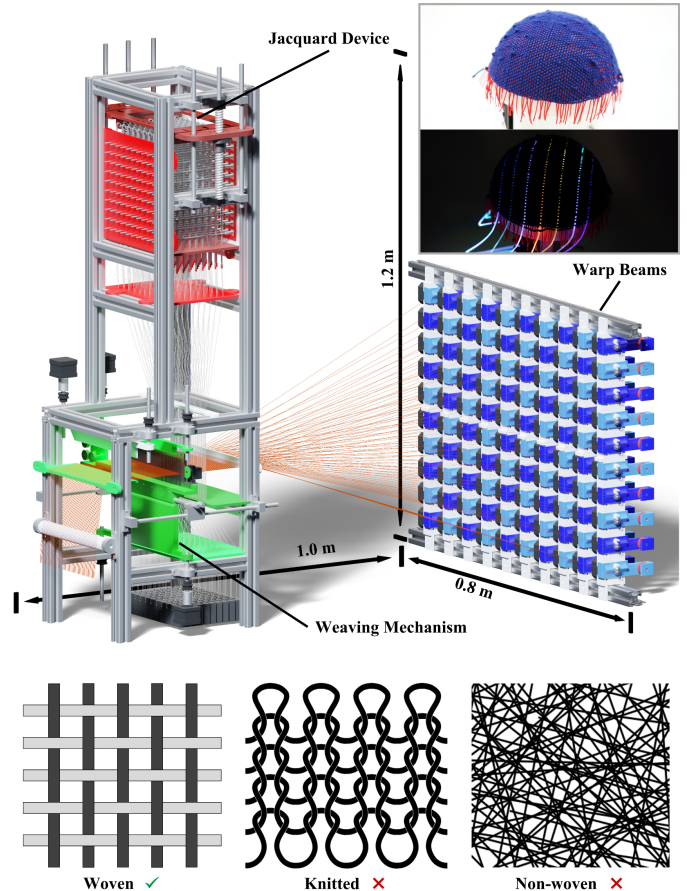


Fig. 1. The overview of our 3D surface weaving system, where there are three hardware components namely 1) jacquard device, 2) warp beams, and 3) weaving mechanism. Different fabric forming choices are given in the bottom row, among which we choose weaving so that the non-traditional materials with high bending-stiffness can be employed more easily. An example weaving result as a hemisphere with embedded optical fibres has been shown in the right-upper corner.

fabric is completely filled with stitches but the map for a 3D surface is only filled partially (see Fig.2(b) for an example). Such a map is called a weaving map. Weaving process results in interlaced warp and weft threads that are perpendicular to each other [1].

Three-dimensional shape can be formed in knitting by the operations to increase or decrease the number of stitches, which is commonly adopted in hand knitting for simple shapes such as a rounded cap since the middle of 16th century [19]. Different from weaving, the interlooped stitches in knitting are formed by warping a continuous filling thread throughout the whole fabric-forming process. More complicated geometry was considered in computer graphics by employing increase-decrease shaping for hand knitting [10] or short-row shaping

*Corresponding authors: Charlie C.L. Wang and Yeung Yam (E-mail: changling.wang@manchester.ac.uk; yyam@mae.cuhk.edu.hk)

¹X. Chen and Y. Yam are with the Dept. of Mechanical and Automation Engineering, The Chinese University of Hong Kong, Hong Kong, China.

²X. Chen, L.M. Lai, Z. Liu, I.C.W. Leung, and Y. Yam are with the Centre for Perceptual and Interactive Intelligence (CPII) Limited, Hong Kong, China.

³C.C.L. Wang is with the Department of Mechanical, Aerospace, and Civil Engineering, The University of Manchester, United Kingdom.

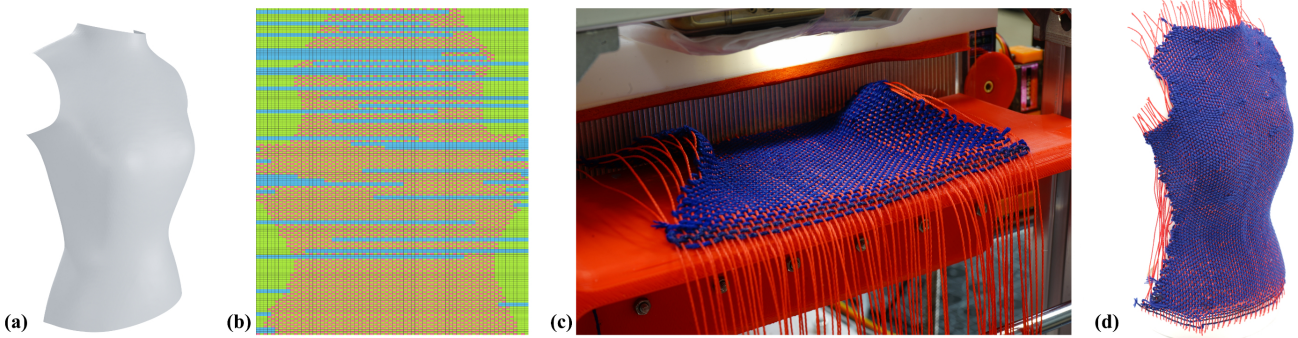


Fig. 2. Given the 3D surface of a vest's front piece (a), our software can generate the weaving information (as the weaving map shown in (b)) for controlling the operations of partial weaving (c). The result of fabrication (d) by cotton threads – red for warp threads and blue for weft threads.

for machine knitting [20]. Increase / decrease shaping changes the local width of the fabric by adding an extra loop in a row of stitches (or trapping a loop to more than one loop in the previous row). Short-row shaping changes the local height of the fabric by knitting partial rows in regions needing more stitches. Modern computational techniques have been developed for automatic knitting maps generation to realize desired shapes, including the compiler [7], the visual programming tool [21], and the algorithm for controlling the distribution of elasticity [20]. However, highly curved loops formed in knitting make it very challenging to use non-traditional materials with high bending-stiffness. Alternative manufacturing methods for fabrics with 3D freeform shapes need to be developed.

In this paper, we propose a new computer-controlled weaving system (see Fig.1) that enables the fabrication of woven fabrics as 3D freeform surfaces. Different from the most existing works on weaving 3D solid geometry like height-fields (ref. [22]), the 3D surface weaving technique introduced in our work focuses on producing 3D surface geometry. Actually, 3D surface weaving is not a blind spot but wildly appears in our daily life, which however usually appears in hand-made products (e.g., woven baskets and woven chairs). Ren et al. [13] presented an optimization-based approach to solving the inverse design problem for woven structures by an algorithm to compute the ribbon's planar geometry. Again, the computer-controlled manufacturing has not been considered yet. When a piece of woven fabric can be fabricated from threads with high bending-stiffness on a computer-controlled machine, it enables many applications in mechatronics by using threads with different materials such as carbon fibres, optical fibres and conductive wires (ref. [4]–[6]).

II. WEAVING 3D FREEFORM SURFACE

This work is motivated by generalizing the short-row based shaping technique, which was originally designed for knitting, on a newly designed weaving machine. Not only the new hardware but also the new software are needed to enable this challenging technology for 3D surface weaving.

First of all, realizing the short-row shaping principle on a weaving machine is easier than the increase-decrease shaping. Specifically, the jacquard device on a weaving machine can be modified to enable the function by controlling the weft

thread (i.e., moving along the row direction) to turn at different locations of the regularly aligned warp threads (i.e., those along the column direction). As a result, different numbers of warp threads can be woven by the weft thread starting from / ending at different locations (see Fig.2(c) for an example).

Secondly, considering that the shape of 3D woven fabric is determined according to the lengths of the warp threads in different columns, the warp threads are required to be individually controlled to ‘pull’ or ‘release’. A matrix of individually controlled warp beams are developed for this function (see the right of Fig.1).

Lastly, how to effectively form the desired pulling operation while keeping the warp threads tight all the time during weaving is the most difficult part when comparing with the traditional planar weaving machines. A weaving mechanism is designed for this purpose. Details will be introduced in Sec. III-C. Therefore, the hardware of our 3D weaving system is compound of the jacquard device, the matrix of warp beams and the new weaving mechanism.

The software of the 3D surface weaving system is also developed to generate weaving maps (e.g., Fig.2(b)) for controlling the operations of 3D surface weaving. Each map is later converted into a set of operations defined as W-code to govern the machine weaving. Both the hardware and the software of our system are designed for realizing the short-row shaping technique on a weaving machine. To the best of our knowledge, no existing approach is available in literature.

In summary, the technical contributions of our work include:

- 1) a method for three-dimensional surface weaving that can use warp and weft threads in high bending-stiffness;
- 2) the novel mechanical design of a computer-controlled system for 3D surface weaving;
- 3) a software solution that can convert a given 3D freeform surface into the corresponding weaving operations (defined as W-code) with the help of the short-row knitting map generation method.

The performance of our technology has been tested and verified on a variety of 3D freeform surfaces. Its functionality in mechatronics applications has been demonstrated by woven surfaces with embedded conductive threads and optical fibres.

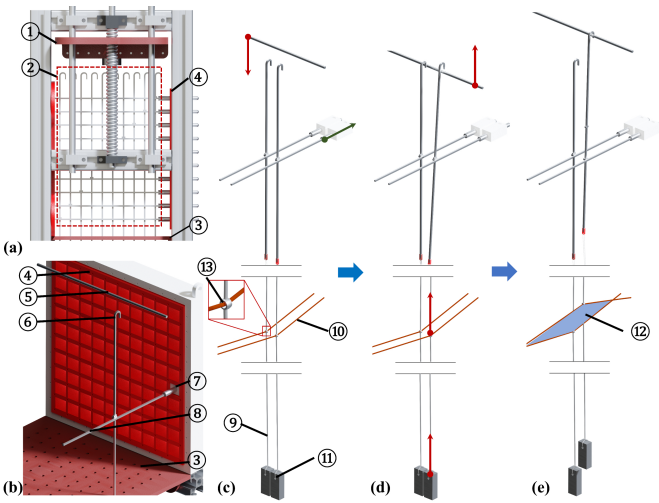


Fig. 3. The jacquard device (a) contains a lifting platform ① equipped with 10 knives ⑤ and a compact hook matrix ② connected with 100 heddle threads ⑨. From the isometric view (b), we can find that each unit of the hook matrix has a hook ⑥ hanging on a needle ⑧ connected with an electronic solenoid ⑦. All the units are installed in an organizer ④. Every hook moves through a hole ③ on the tug board and a heddle thread is fixed at the lower side of the hook. The heddle thread intersects with the warp thread ⑩ through a ring ⑬ that the warp thread can be lifted and dropped to form a shed – see the cross-section shown as ⑫. A weight ⑪ is tied to the end of the heddle thread to drop the warp thread ⑩ through the ring. The parsing motions of two heddle lifters with drop and lift commands are shown in (c)-(e), namely (c) the initial state, (d) the hanging-up state, and (e) the lifted state.

III. HARDWARE DESIGN

We introduce the hardware design of our 3D surface weaving system in this section. The prototype of our machine aims at the application in small domestic workshops. Therefore, the following design parameters are adopted. The dimensions of our hardware are 1.0m (length) \times 0.8m (width) \times 1.2m (height) – see also Fig.1. The maximal width of fabrics is designed as 198mm that are formed by 100 warp threads with a fixed stitch width as 2mm. The length of woven fabrics is theoretically unlimited, and the stitch length can be specified and controlled by our computer program with the limit of a minimal length influenced by the materials of weft threads.

A. Jacquard device

A jacquard device is employed in our system to selectively lift warp threads so that a shed can be formed to allow the shuttle holding weft thread to travel through. Such a device is commonly found in traditional weaving machines to realize embossed patterns on woven fabrics. The modified jacquard device in our system can help to introduce short-row shaping on a weaving machine. Specifically, only the selected warp threads will be lifted to form a shed with their neighboring threads so that they can be involved in the woven structure by interweaving with the weft thread.

As illustrated in Fig.3, a lifting platform with 10 knives is driven by a pair of screws to move up and down to lift (or drop) the selected heddle threads synchronously (the red arrow in Fig.3(c) and (d)). Each hook can be individually controlled by a push (or pull) motion (the green arrow in Fig.3(c)) with the help of an handle connecting to an electronic solenoid

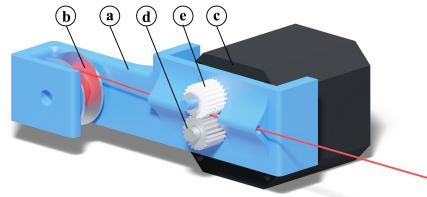


Fig. 4. Each warp beam is compound of a frame ④, a coil of warp thread ⑤, a motor ⑥, and a pair of driving gears ⑦ and ⑧.

installed in an organizer. This controls whether a hook will be hanged on the corresponding knife to move together. The solenoid can become shorten when receiving a command from a control program. As a result, the attached needle will help position the corresponding hook to the location to be lifted by a knife.

The parsing motions are given in Fig.3(c)-(e) to illustrate how to form a shed by two hooks holding two neighboring warp threads. In this example, the right hook is selected to lift its connected warp thread while the left hook keeps dropping. First of all, the hooks are all hanging on their corresponding needles when the lifting platform is at a higher level in the initial state (see Fig.3(c)). When a command is received, the lifting platform moves down to the height where the hooks can hang over the knives by shortening the the solenoids to move the needles (as illustrated as green arrow in Fig.3(c)). After pulling the right hook to the hanging position (as Fig.3(d)), the lifting platform moves up to its previous position. As a result, the knife has lifted the right hook and also the connected warp thread. A shed is formed by the lifted warp thread and the warp thread held by the left hook (see Fig.3(e)).

B. Warp beams

Different from the planar weaving machines, all warp threads in our system can be individually released and pulled by the warp beams installed at the back of the whole machine (see Fig.1). As a result, the length of each warp thread can be precisely controlled to form the desired 3D shape of fabric.

The mechanical structure of a warp beam is show in Fig.4. A warp thread released from the coil travels through two spacing holes where the warp thread is held by a pair of driving gears. The release and pull motions on the warp thread are precisely controlled by the pair of driving gears and the engaged step motor.

C. Weaving mechanism

As the most important hardware component of our system, the weaving mechanism has more parts and involves more complicated motions. After forming the shed by the jacquard device and releasing the threads by the warp beams, the weaving machine needs to complete the rest operations for the 3D surface weaving – i.e., forming required woven structures on the fabric.

Weaving mechanism of our 3D weaving machine is similar to the traditional flat machine but has a special function of pushing the newly formed woven structures to the previous rows along the columns that the woven structures are skipped

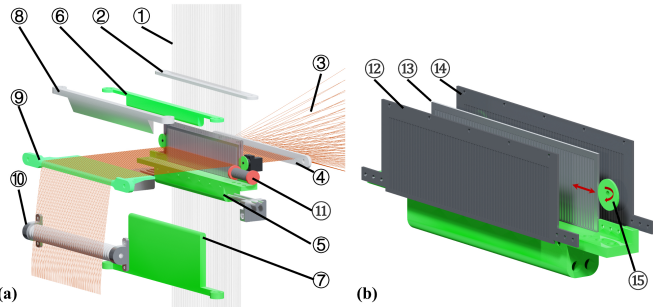


Fig. 5. A novel weaving mechanism (a) is invented in our system to form required deformation on the fabric by operating the following components together: ① the heddle threads connected to the jacquard device through ② the heddle board, ③ the warp threads held by the warp beams through ④ the warp board, ⑤ the reed with three pieces of blades, ⑥ & ⑦ as a pair of warp limiters, ⑧ a fabric clamp, ⑨ a fabric collection platform, ⑩ a fabric beam, and ⑪ the shuttle holding the weft thread. Specifically, the front piece ⑫ and the back piece ⑭ of the reed are fixed while the middle piece ⑬ can shift a bit along the weft direction driven by a pair of eccentric wheels ⑮.

(according to the designed weaving map). This function is jointly realized by the new reed design with three pieces and the weaving motions for shifting the different lengths of threads (released by the warp beams according to the designed weaving map) from the beam side to the fabric side. The components of our machine and the detailed structure of the reed with three pieces of blades have been shown in Fig.5. Besides of the reed, other important components include the limiters and the fabric clamp. The two limiters work like a ‘sliding door’ that moves up and down. When the ‘door’ is closed, all warp threads are limited at the same level. Located above the collection platform, the fabric clamp can move down to press and hold the already completed woven structures on the fabric.

The parsing motions for weaving a row of woven stitches are explained below with the help of Fig.6.

- After weaving one row (see Fig.6(a)), we are about to lift / drop the heddle threads to realize a new jacquard pattern of warp threads according to the second row of the weaving map. The resultant up / down states of warp threads are as shown in Fig.6(b). At the same time, we release the warp threads by the warp beams according to the pattern shown in the second row of the weaving map.
- The reed is placed at a location near to the heddle board while the limiters are open and the fabric clamp presses the fabric on the collection platform. This forms a shed with the largest area to ease the travel of shuttle that carries the weft thread moving from one side to the other side of the loom (see Fig.6(c, d)).
- After the shuttle’s travel, woven structures of the second row in the weaving map have been formed on the fabric but in a loose way. We move the reed to the middle position that is slightly ahead of the limiters (see Fig.6(d, e) – indicated by the red arrow).
- The limiters are then closed to ensure all warp threads being clamped at the same height before catching them by the reed (see the change from Fig.6(e) to (f) – indicated by the blue arrows). Meanwhile, the loosely formed woven structures are ‘pushed’ onto the previously

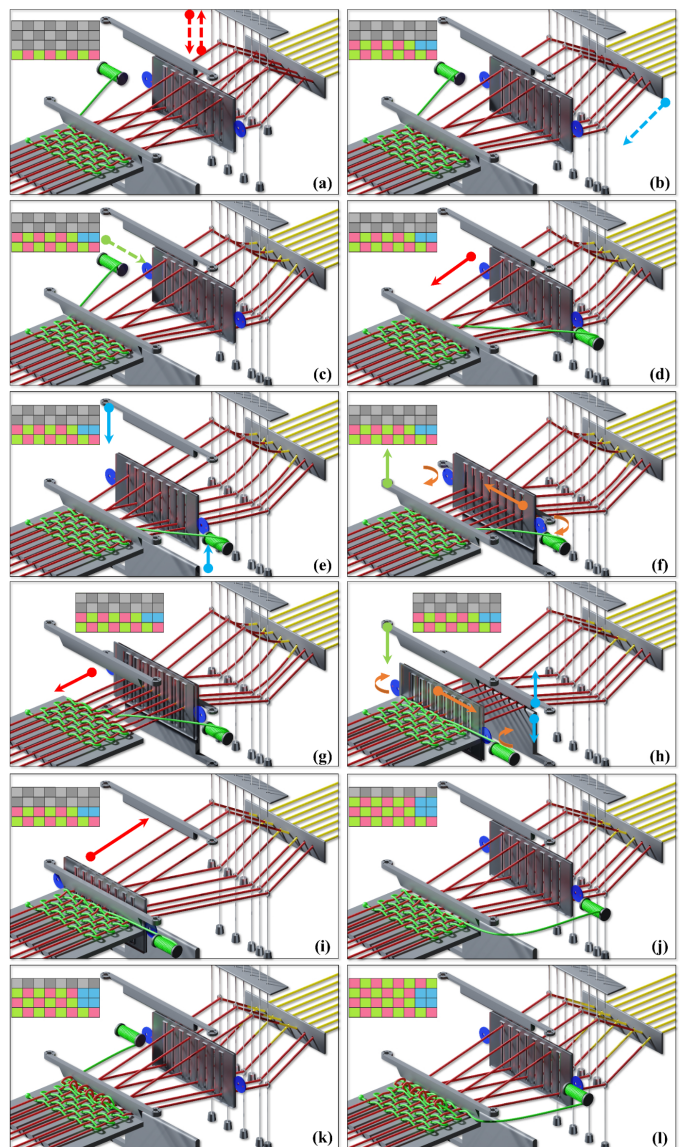


Fig. 6. The change of the woven fabric and the configurations of the weaving machine while fabricating a few rows as indicated by the weaving map: (a) the status after weaving the first row, (b-i) the parsing motions for weaving the second row, (j, k) the states when and after weaving the third row, and (l) the state after weaving the fourth row.

produced fabric by 1) shifting the middle blade of the reed to hold all warp threads (Fig.6(f)), 2) lifting up the fabric clamp (Fig.6(f, g)), and 3) tightening the loosely formed woven structures by pushing the reed forward to the position below the fabric clamp (Fig.6(g)).

- Lastly, as shown in Fig.6(h), the fabric clamp is dropped to hold the newly formed stitches on the fabric (indicated by the green arrow), the reed releases the warp threads (shown by the orange arrows), and the limiters are opened (see the blue arrows). The reed is moved back to the initial position to be ready for weaving the next row (Fig.6(i, j)).

The above motions are repeated for every row to complete the weaving process of all rows – e.g., see Fig.6(j, k) for the third row and Fig.6(l) for the fourth row. As a result, the woven fabric with designed 3D shape can be obtained.

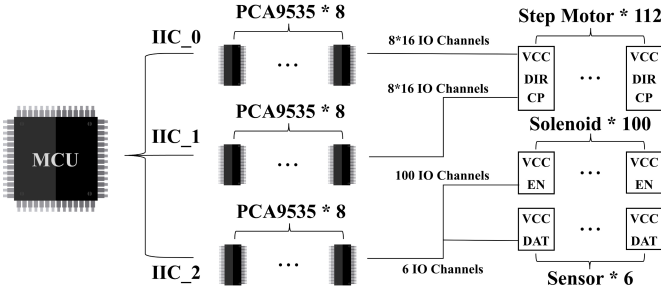


Fig. 7. The schematic of the control system used in our approach.

D. Control system

There are 112 step motors (100 for warp beams, 1 for the jacquard device, and 11 for the weaving mechanism), 100 electronic solenoids (for the warp threads), and 6 position sensors employed in our 3D surface weaving system. It is important to control these actuators and sensors in a stable and synchronized way. Since over 300 IO channels are required, the IO extension chip (i.e., PCA9535) is employed to connect the sensors / actuators to the *Micro Control Unit* (MCU – i.e., F103ZET6) through the *Inter-Integrated Circuit* (IIC). The schematic is as shown in Fig.7, where we use three sets of IIC to communicate with 24 PCA9535 to complete the control tasks – considering that the maximal number of chips for each IIC is 8. The firmware of our control system was developed by C programming language and all circuits are designed by using EasyEDA. Detailed schematics and PCB layout can be accessed at: [\[Charlie:: mfff.pdf\]](#).

IV. SOFTWARE AND MACHINE CODE

Given a 3D freeform surface to be fabricated by our weaving machine, we first generate a short-row based knitting map with the help of stitch meshes. After that, the knitting map will be converted into machine code including both the information of jacquard pattern and the machine code for weaving operations.

A. Short-row based knitting map generation

The method presented in [20] was employed in our system to generate short-row based knitting maps. A geodesic distance-field is first computed from the user-defined source (point or curve) on the input surface, where the isocurves of the field with the distance as the target stitch height are extracted to serve as the boundaries of rows of stitches. The isocurves are then sampled into segments with length equal to the target stitch width. Lastly, the stitch meshes are constructed by connecting segments on neighboring isocurves with optimized quadrangles / triangles. The following rules are applied to generate the knitting maps considering manufacturing constraints:

- 1) The stitches are organized row by row;
- 2) All stitches in the same row are neighboring connected;
- 3) Stitches in the same row are formed in an alternating left-to-right and right-to-left order;
- 4) The ending stitch of the current row should be neighboring to the starting stitch of the next row.

The stitch mesh generated by the algorithm of [20] can satisfy all these requirements. As a result, every stitch can be mapped

to a location in the 2D knitting map by its index of the row and its location (i.e., order) in the row – see Fig.8(b) and (c) for an example.

A knitting map presents the operational information about how to form stitches while traveling in the alternated left-to-right and right-to-left ways by the carriers holding yarns. Three different blocks are shown in different colors as colorful (e.g., cyan / yellow in Fig.8(c)), white, and gray. The colorful blocks in a knitting map are the stitches formed by loops of yarns, where the cyan ones are stitches formed by the carrier travelling from right to left and the yellow blocks represent those formed by traveling from left to right. No stitch will be formed for the white or the gray blocks. That means the carrier will *not* travel into the white / gray regions. Due to the short-row shaping technique, the stitches below and above the gray blocks would be connected to change the height of the local fabric – therefore, a 3D surface can be produced on woven structures.

B. Converting knitting map into weaving code

Different from knitting, every stitch of the woven structure is formed together by two neighboring warp threads and the other two neighboring weft threads. Therefore, for a knitting map $K(\cdot)$ with N rows and M columns, it will be converted into a weaving map W with $M+1$ columns and $N+1$ rows. When fabricating the i -th row of the woven structure, $W_{i,j}$ indicates the Jacquard configuration of the j -th warp thread and the operation of the corresponding warp beam holding this thread.

Unlike the short-row shaping technique of knitting that the travel of carrier are only conducted in a limited range for each row (e.g., only the region with yellow or cyan blocks in Fig.8(c)), the carrier holding the weft thread always travels from the head to the tail of each row on our weaving machine. When two neighboring warp threads have the same Jacquard configuration (i.e., both up or both down as $W_{i,j} = W_{i,j+1}$), no woven structure can be formed.

On the other aspect, two results can be obtained by using different operations of the warp beam for the j -th thread when $W_{i,j} = W_{i+1,j}$:

- If the beam releases the j -th thread with a unit length (i.e., row distance) as usual, it will become a floating thread between the i -th row and $(i+1)$ -th row;
- If the beam keeps holding the thread, the already formed woven stitch before the i -th row will be tightly ‘sewn’ to the later stitch after the $(i+1)$ -th row.

The first situation happens for the white regions in the knitting map, and the second configuration is corresponding to the gray regions of a knitting map.

An algorithm is developed to generate $W(\cdot)$ from $K(i,j)$ with $i = 1, \dots, N$ as row index starting from bottom and $j = 1, \dots, M$ as column index starting from left. For the sake of explanation, colors are used while introducing the algorithm below.

- **Step 1:** Create a new weaving map as $W(i,j)$ with $N+1$ rows and $M+1$ columns and fill all blocks of $W(i,j)$ by green.

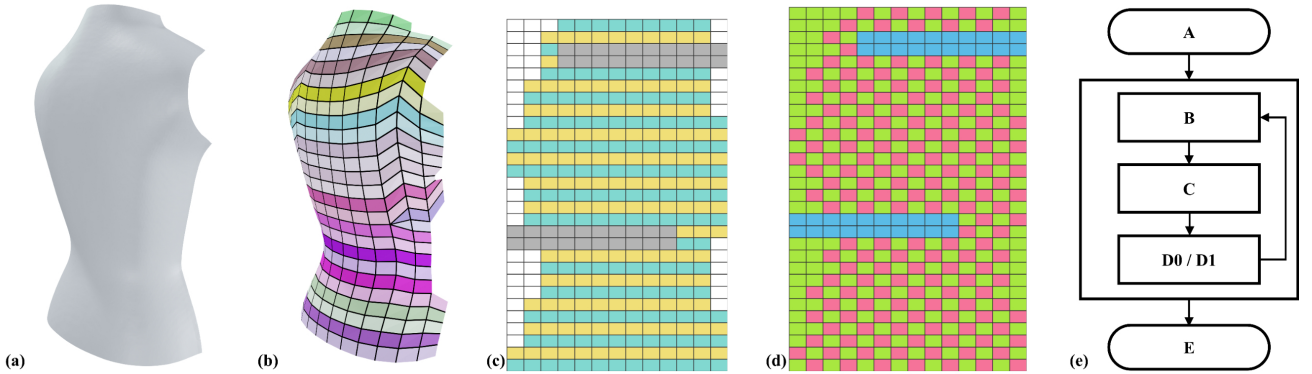


Fig. 8. Given a target surface (a), a stitch mesh for short-row shaping based knitting [20] can be generated as shown in (b). The stitch mesh can be converted into (c) a knitting map, which is converted into a weaving map (d) and the machine code (e) to supervise the operations of our weaving machine.

- **Step 2:** We check the color of every block $K(i, j)$ in the knitting map so that 1) we assign $W(i+1, j)$ as magenta when $K(i, j)$ is yellow or cyan or 2) $W(i+1, j)$ is assigned as blue when $K(i, j)$ is gray.
- **Step 3:** For every row $W(i, \cdot)$ ($i \neq 1$), if the last non-green block is located at $W(i, j')$, we assign $W(i, j' + 1) = W(i, j') -$ i.e., one column is extended.
- **Step 4:** For the first row $W(1, \cdot)$, we copy it from the second row as $W(1, j) = W(2, j)$ for every block.
- **Step 5:** For a magenta block $W(i, j)$, we convert its color to green when 1) both i and j are odd numbers or 2) both i and j are even numbers.

At the end of this algorithm, we generate a weaving map with both the Jacquard information and the warp beam information. Specifically, we have

- 1) $W(i, j) = \text{blue}$: the j -th warp beam will not release the warp thread and the Jacquard pattern of the j -th warp thread is not changed;
- 2) $W(i, j) = \text{magenta}$: the j -th warp beam will release the thread for a unit length and the Jacquard pattern of the j -th thread is changed to ‘up’ if it is not;
- 3) $W(i, j) = \text{green}$: the j -th warp beam will release the thread and the j -th thread is dropped to the ‘down’ status for its Jacquard pattern.

Based on the above definitions for the color configurations, we convert the weaving map into a *W-code* file with a structure as shown in Fig.8(e) to supervise the operations of our 3D surface weaving machine. The syntax of *W-code* consists of five commands:

- **A:** The initialization command to reset the hardware for the coming weaving process as Fig.6(a).
- **B:** The command is given together with $M + 1$ binary numbers to instruct the jacquard device selectively lifted the warp threads as Fig.6(b).
- **C:** A command followed by $M + 1$ binary numbers is used to instruct the warp beams for selectively releasing the corresponding warp threads (e.g., Fig.6(c)), where the unit length of release can be specified by users in advance.
- **D:** A command followed by a boolean value to drive the shuttle (i.e., D0 – from left to right and D1 – from right to left) and to completed the weaving operation of one row as described in Fig.6(d)-(i).

TABLE I
STATISTICS OF COMPUTATION

Model	Trgl. Num.	Fig.	Thread Num. [†]		Comp. Time [‡] (sec.)	
			Weft	Warp	Knit M.	W-Code
Hemisphere	4,000	1	138	72	1.64	0.38
		-	276	144	1.67	1.71
Vest (Front)	26,593	2	170	71	1.78	0.49
		-	340	142	7.01	2.01
Vest (Back)	28,763	9	173	72	1.97	0.52
		-	346	144	7.75	2.19
Triple-Peak	10,016	9	190	58	0.97	0.45
		-	380	116	3.85	1.98

[†] The tests were conducted to demonstrate the scalability of our software – the maximally allowed warp thread # on our prototype machine is 100.

[‡] The computing time of W-code generation includes both the step of weaving map generation and the step for converting it into W-code.

- **E:** The end command for stopping the weaving process. An example W-code file for the weaving map shown in Fig.8(d) can be found in the supplementary document.

V. RESULTS

We have made a prototype machine by off-the-shelf electrical / mechanical components, motors and 3D printed parts, and the software of our system was developed by Python. The experimental tests reported in this section were run on a desktop PC with AMD Ryzen 7 5800X 3.8GHz CPU and 32GB RAM. Different materials are employed to fabricate examples with a variety of freeform 3D shapes.

A. Statistics of computation and fabrication

The results of experimental tests conducted on our prototype system are quite encouraging although both the hardware and the software can be further optimized.

The statistics of computation are shown in Table I, where the results with two different resolution of threads are computed. As it can be observed, all examples can be completed within 10 sec. and the major bottleneck is the step of knitting map generation [20]. The complexity of computation is $O(AB \log B)$ (caused by the knitting map generation algorithm) with A and B being the number of stitches along the warp and the weft directions respectively.

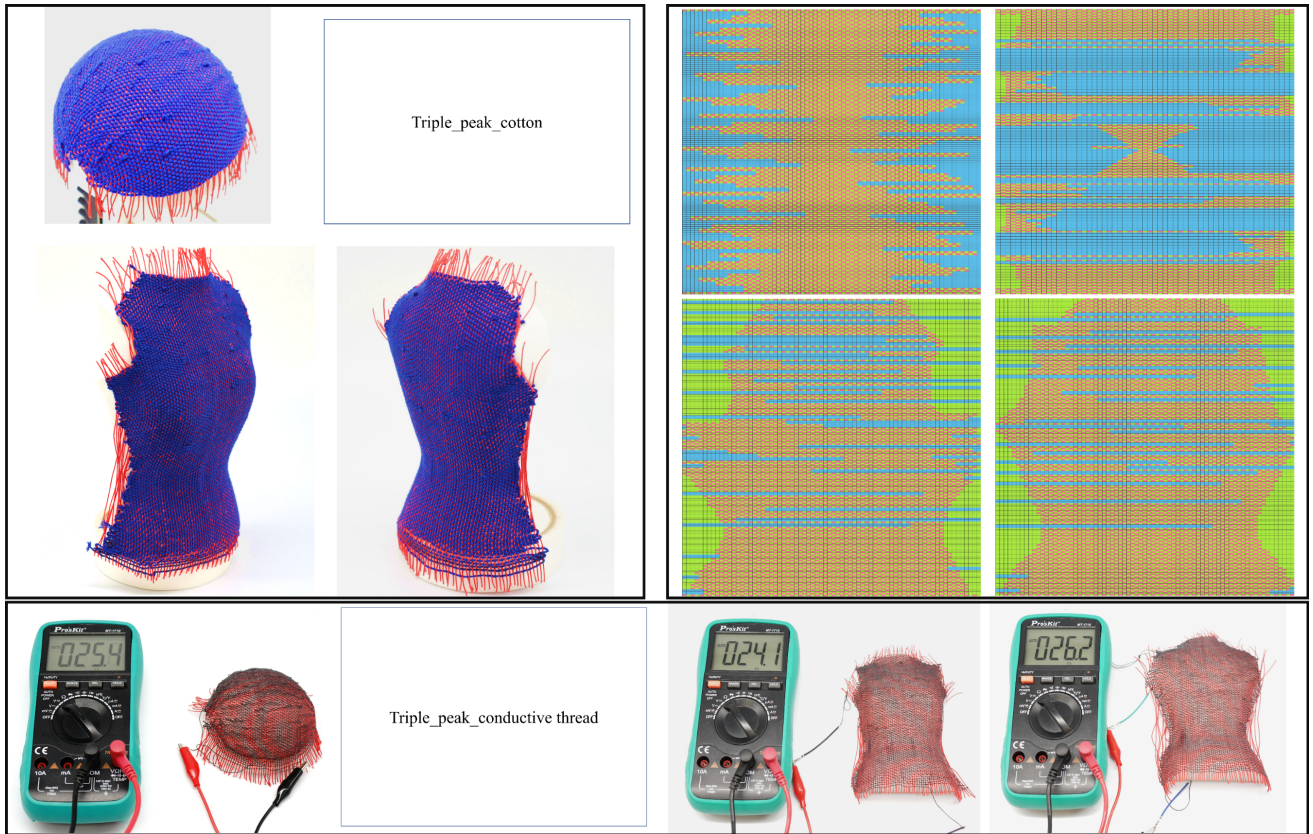


Fig. 9. The results of physical specimens fabricated by our 3D surface weaving machine on four different examples (a), where their corresponding maps of weaving are given in (b). Our weaving system enables the flow of electric current over the freeform surfaces of fabrics by using conductive threads in (c).

TABLE II
STATISTICS OF PHYSICAL WEAVING

Model	Thread #		Materials		Weaving Time (min.)
	Weft	Warp	Weft	Warp	
Hemisphere	138	72	Cotton	Cotton	140
			Conductive	Cotton	152
			Cotton	Hybrid	145
			Hybrid	Cotton	158
Vest (Front)	170	71	Cotton	Cotton	170
			Conductive	Cotton	181
			Cotton	Hybrid	173
			Hybrid	Cotton	193
Vest (Back)	173	72	Cotton	Cotton	174
			Conductive	Cotton	183
Triple-Peak	190	58	Cotton	Cotton	195
			Conductive	Cotton	211

We have physically produced these example models on our prototype of the 3D surface weaving machine by using different materials (see Fig.9), where the warp threads are waxed threads with cotton core and the cotton thread (waxed) and the conductive threads (bare copper with silicone rubber insulation) are used for weft threads. All models can be fabricated within a reasonable time, where the statistics have been listed in Table II. We also tested the examples by replacing a few warp threads by optical fibres – named as ‘hybrid’ warp threads in Table II with the results shown in Figs. 1 & 10. By using the in-lay technique [23], we can also ‘insert’ a few optical fibres along the weft direction – named as ‘hybrid’ weft threads in Table II with the results shown in Fig.10.

Note that the in-lay fabrication needs manual operations on our prototype machine although it has the potential to be automated by robotic techniques (e.g., [24], [25]).

B. Applications in mechatronics

As a mechatronic system, our 3D surface weaving can help produce more interesting applications in mechatronics. When conductive threads are used as already shown in Fig.9(c), our 3D surface weaving approach enables the flow of electric current over the freeform surfaces of fabrics so that they can work like soft PCBs. This has many potential applications such as functional garments [26], motion sensing [27], and ‘skin’ of cobot [28]. We plan to apply our surface weaving technology to develop some new applications along this thread of research.

Besides of conductive threads, we have also employed optical fibres to weave fabrics with 3D freeform surfaces (as shown in Fig.10). The lighting results with different combinations of lights / fibres have demonstrated the potential application of soft display on fabrics (ref. [29]). In our future research, we will further investigate the techniques to control the location and the pattern of optical fibres more precisely.

VI. CONCLUSION

This paper presents a new computer-controlled weaving system, which is the first approach that automates the fabrication of 3D freeform woven fabrics by using threads in non-traditional materials with high bending-stiffness. The major



Fig. 10. Examples to demonstrate the functionality of 3D surface weaving by optical fibres, where the fibres can be either employed as (top and middle rows) warp threads or (bottom row) weft threads (by the in-lay technique).

contributions of this work comes from both the mechatronics system design and the software algorithms to enable the computer-controllable weaving process. The performance of our technology has been tested and verified on a variety of 3D freeform surfaces and applications.

One major limitation of the current prototype system is that the movement of shuttle and the insertion of the additional weft threads in different materials are not fully automated yet – i.e., a certain level of manual operations are required although the effort needed is minor. Also, the weaving speed of our prototype machine is much slower than those flat weaving machines used in industry. Lastly, the abrasion of warp threads caused by the reed's motion requires the threads being waxed to prevent the damage of its ‘core’.

REFERENCES

- [1] S. Adanur, *Handbook of weaving*, CRC press, 2020.
- [2] A. D. Kelkar, J. S. Tate, and R. Bolick, “Structural integrity of aerospace textile composites under fatigue loading,” *Materials Science and Engineering: B*, vol. 132, no. 1-2, pp. 79–84, 2006.
- [3] M. Di Renzo, F. Rizzo, G. Parati, G. Brambilla, M. Ferratini, and P. Castiglioni, “Magic system: A new textile-based wearable device for biological signal monitoring, applicability in daily life and clinical setting,” in *2005 IEEE engineering in medicine and biology 27th annual conference*, pp. 7167–7169, IEEE, 2006.
- [4] A. P. Mouritz, M. K. Bannister, P. Falzon, and K. Leong, “Review of applications for advanced three-dimensional fibre textile composites,” *Composites Part A: applied science and manufacturing*, vol. 30, no. 12, pp. 1445–1461, 1999.
- [5] A. Komolafe, B. Zaghari, R. Torah, A. S. Weddell, H. Khanbareh, Z. M. Tsikriteas, M. Vousden, M. Wagih, U. T. Jurado, J. Shi, et al., “E-textile technology review—from materials to application,” *IEEE Access*, vol. 9, pp. 97152–97179, 2021.
- [6] A. Levitt, D. Heigh, P. Phillips, S. Uzun, M. Anayee, J. M. Razal, Y. Gogotsi, and G. Dion, “3D knitted energy storage textiles using mxene-coated yarns,” *Materials Today*, vol. 34, pp. 17–29, 2020.
- [7] J. McCann, L. Albaugh, V. Narayanan, A. Grow, W. Matusik, J. Mankoff, and J. Hodgins, “A compiler for 3D machine knitting,” *ACM Transactions on Graphics (TOG)*, vol. 35, no. 4, pp. 1–11, 2016.
- [8] V. Narayanan, L. Albaugh, J. Hodgins, S. Coros, and J. McCann, “Automatic machine knitting of 3D meshes,” *ACM Transactions on Graphics (TOG)*, vol. 37, no. 3, pp. 1–15, 2018.
- [9] Y. Liu, L. Li, and P. F. Yuan, “A computational approach for knitting 3D composites preforms,” in *The International Conference on Computational Design and Robotic Fabrication*, pp. 232–246, Springer, 2019.
- [10] Y. Igarashi, T. Igarashi, and H. Suzuki, “Knitting a 3D model,” in *Computer Graphics Forum*, vol. 27, pp. 1737–1743, Wiley Online Library, 2008.
- [11] K. Bilisik, “Multiaxis 3D weaving: Comparison of developed two weaving methods (tube-rapier weaving versus tube-carrier weaving) and effects of bias yarn path to the preform properties,” *Fibers and Polymers*, vol. 11, no. 1, pp. 104–114, 2010.
- [12] R. Wu, C. Harvey, J. X. Zhang, S. Kroszner, B. Hagan, and S. Marschner, “Automatic structure synthesis for 3D woven relief,” *ACM Transactions on Graphics (TOG)*, vol. 39, no. 4, pp. 102–1, 2020.
- [13] Y. Ren, J. Panetta, T. Chen, F. Isvoranu, S. Poincloux, C. Brandt, A. Martin, and M. Pauly, “3D weaving with curved ribbons,” *ACM Transactions on Graphics*, vol. 40, p. 127, 2021.
- [14] X. Chen, *Advances in 3D textiles*, Elsevier, 2015.
- [15] B. Shirinzadeh, G. Alici, C. W. Foong, and G. Cassidy, “Fabrication process of open surfaces by robotic fibre placement,” *Robotics and Computer-Integrated Manufacturing*, vol. 20, no. 1, pp. 17–28, 2004.
- [16] B. Shirinzadeh, G. Cassidy, D. Oetomo, G. Alici, and M. H. Ang Jr, “Trajectory generation for open-contoured structures in robotic fibre placement,” *Robotics and Computer-Integrated Manufacturing*, vol. 23, no. 4, pp. 380–394, 2007.
- [17] L. Sorrentino, M. Marchetti, C. Bellini, A. Delfini, and F. Del Sette, “Manufacture of high performance isogrid structure by robotic filament winding,” *Composite Structures*, vol. 164, pp. 43–50, 2017.
- [18] H. Li, S. Sueda, and J. Keyser, “Computation of filament winding paths with concavities and friction,” *Computer-Aided Design*, vol. 141, 2021.
- [19] D. J. Spencer, *Knitting technology: a comprehensive handbook and practical guide*, CRC press, 2001.
- [20] Z. Liu, X. Han, Y. Zhang, X. Chen, Y.-K. Lai, E. L. Doubrovski, E. Whiting, and C. C. Wang, “Knitting 4D garments with elasticity controlled for body motion,” *ACM Transactions on Graphics (TOG)*, vol. 40, no. 4, pp. 1–16, 2021.
- [21] V. Narayanan, K. Wu, C. Yuksel, and J. McCann, “Visual knitting machine programming,” *ACM Transactions on Graphics (TOG)*, vol. 38, no. 4, pp. 1–13, 2019.
- [22] R. Wu, C. Harvey, J. X. Zhang, S. Kroszner, B. Hagan, and S. Marschner, “Automatic structure synthesis for 3D woven relief,” *ACM Trans. Graph.*, vol. 39, aug 2020.
- [23] K. Searle, “The rigid heddle - inlaid weaves,” *Minnesota Weaver*, vol. 3, no. 5, 1978.
- [24] V. Petrik, V. Smutný, and V. Kytki, “Static stability of robotic fabric strip folding,” *IEEE/ASME Transactions on Mechatronics*, vol. 25, no. 5, pp. 2493–2500, 2020.
- [25] Y. She, S. Wang, S. Dong, N. Sunil, A. Rodriguez, and E. Adelson, “Cable manipulation with a tactile-reactive gripper,” *The International Journal of Robotics Research*, vol. 40, no. 12–14, pp. 1385–1401, 2021.
- [26] C. Gonçalves, A. F. da Silva, R. Simoes, J. Gomes, L. Stirling, and B. Holschuh, “Design and characterization of an active compression garment for the upper extremity,” *IEEE/ASME Transactions on Mechatronics*, vol. 24, no. 4, pp. 1464–1472, 2019.
- [27] D. Kim, J. Kwon, S. Han, Y.-L. Park, and S. Jo, “Deep full-body motion network for a soft wearable motion sensing suit,” *IEEE/ASME Transactions on Mechatronics*, vol. 24, no. 1, pp. 56–66, 2019.
- [28] G. Pang, G. Yang, W. Heng, Z. Ye, X. Huang, H.-Y. Yang, and Z. Pang, “CoboSkin: Soft robot skin with variable stiffness for safer human–robot collaboration,” *IEEE Transactions on Industrial Electronics*, vol. 68, no. 4, pp. 3303–3314, 2021.
- [29] T. Someya, “Put down that smartphone: The display is on your skin: The screen is the last frontier in stretchable, bendable, body-conforming electronics,” *IEEE Spectrum*, vol. 58, no. 6, pp. 38–43, 2021.

APPENDIX A: DETAILED SCHEMATICS AND PCB LAYOUT

In this appendix, we provide the detailed schematics and PCB layout of our 3D surface weaving machine's control system.

This. [Charlie:: more to add]

APPENDIX B: EXAMPLE W-CODE

We list the example W-code of the back piece of the vest example below, which is corresponding to the weaving map shown in Fig.8(d).

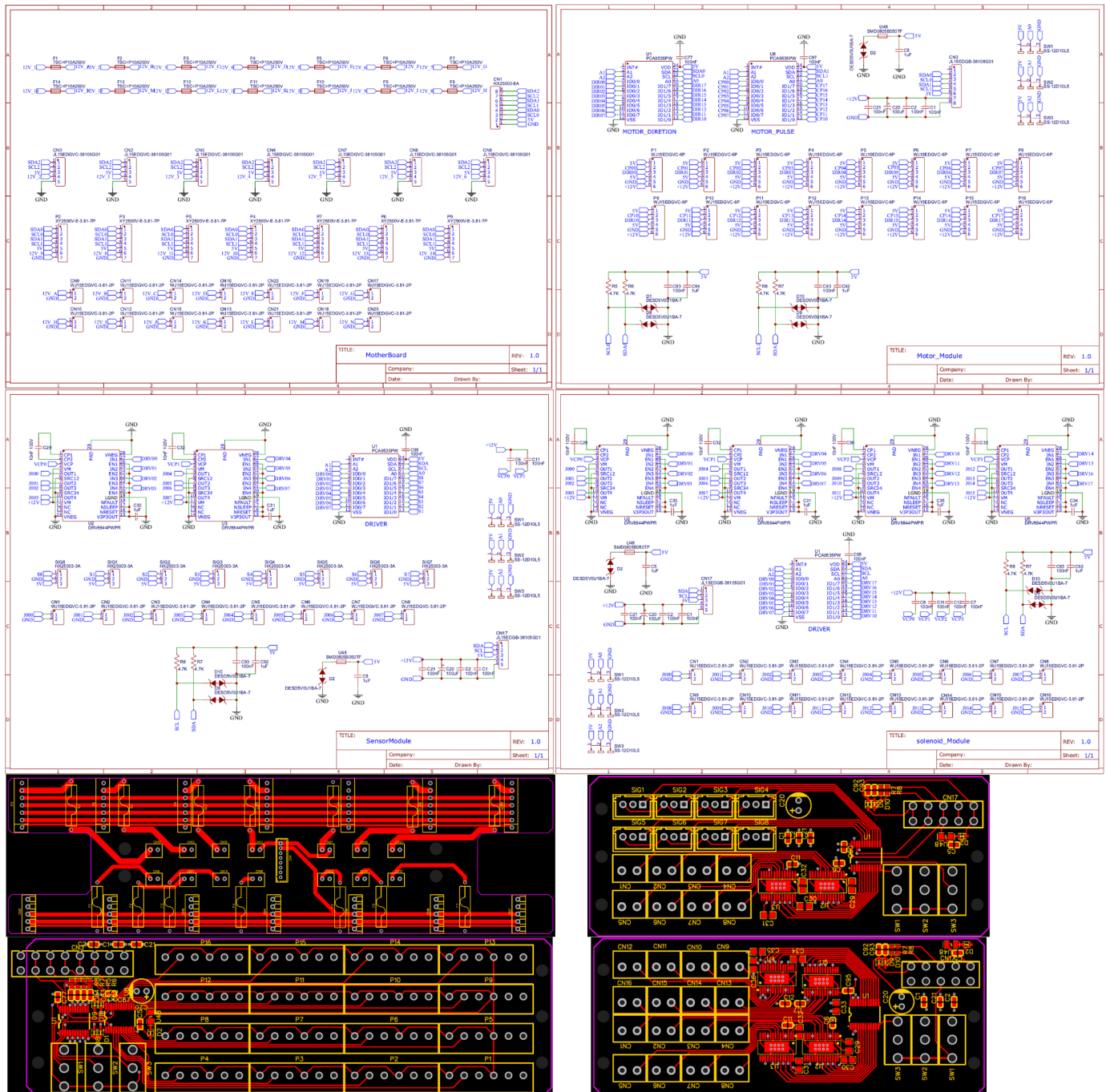


Fig. 11. The detailed schematics and PCB layout for each module.